Journal of Fluorescence (2019) 29:279–291
https://doi.org/10.1007/s10895-018-02338-0

ORIGINAL ARTICLE

Novel 4,4′-Fluoresceinoxy Bisphthalonitrile Showing Aggregation-Induced Enhanced Emission and Fluorescence Turn off Behavior to Fe^{3+} Ions

G. S. Amitha[1] · Vijisha K. Rajan[2] · K. Muraleedharan[2] · Suni Vasudevan[1]

Received: 21 September 2018 / Accepted: 26 December 2018 / Published online: 9 January 2019

Abstract
A novel 4,4′-fluoresceinoxy bisphthalonitrile FPN is synthesized from fluorescein and 4-nitrophthalonitrile by aromatic nucleophilic ipso nitro substitution reaction. The structure of FPN constitutes phthalonitrile-fluorescein-phthalonitrile, acceptor-donor-acceptor, A-D-A form and the solvatochromic study of newly synthesized compound FPN was done in hexane, cyclohexane, $CHCl_3$, DCM, DMF, acetonitrile, ethanol and in methanol. The aggregation behavior of FPN was investigated in good-poor solvent mixture DMF-water in various proportions and the molecule was found to be exhibiting Aggregation Induced Emission Enhancement AIEE for volume percentage of water beyond 50% with a significant hypsochromic shift of 70 nm in the emission maxima from 458 to 388 nm. This phenomenon is termed as Aggregation Induced Blue Shifted Emission Enhancement AIBSEE and was reported in substituted phthalonitrile for the first time. The chemo sensing activity of FPN with various transition metal ions also has been checked by fluorescence spectroscopy where the new molecule FPN exhibited fluorescence turn OFF behaviour towards Fe^{3+} ion in acetonitrile-methanol ACN-MeOH solution. The binding stoichiometry of FPN with Fe^{3+} was verified by Job's plot analysis and Density Functional Theory DFT-B3LYP computational methodology by using Gaussian 09 software.

Keywords 4,4′-fluoresceinoxy bisphthalonitrile FPN · Aggregation induced blue shifted emission enhancement AIBSEE · Substituted phthalonitrile · Chemo sensing · Fe^{3+} ion

Introduction

Fluorophores absorb a wide range of wavelengths of light and they generally emit or fluoresce at a higher wavelength. This property allows to create or develop a large number of luminescent systems to meet the versatile demand of modern technology [1, 2]. A major class of these fluorophores is organic molecules with fused aromatic systems with extended π delocalization. The luminescent properties of the fluorophores in solution could be affected by aggregates formation, which mainly depends on several external factors such as concentration, polarity, nature of the solvent, temperature etc. [3]. In most of the cases, water is referred to as the aggregation causing solvent, on account of the hydrophobic interaction of fluorophores [4]. The natural tendency of luminophores to quench its own fluorescence at high concentration and at solid state by virtue of aggregate formation is termed as Aggregation Caused Quenching (ACQ), as first reported by Foster and Kasper in 1954 [5, 6]. This phenomenon imposes so many restrictions and questions the efficiency and practical utility of fluorescent materials [7] for their vast variety of applications as emitting material (in light emitting diode LED) [8], energy harvesting material (in Organic Solar Cells OSCs) [9], biological probe [10] for cellular imaging in aqueous media etc. But later, in contrast to the ACQ effect, Tang et al. found out a milestone observation of an abnormal phenomenon termed as "aggregation-induced emission" (AIE) as the inherently non-luminescent silole molecules were induced to emit light by aggregate formation [11, 12]. This ultimately

Electronic supplementary material The online version of this article (https://doi.org/10.1007/s10895-018-02338-0) contains supplementary material, which is available to authorized users.

✉ Suni Vasudevan
suniv@nitc.ac.in

[1] Department of Chemistry, National Institute of Technology Calicut, Calicut, Kerala 673601, India

[2] Department of Chemistry, University of Calicut, Calicut, Kerala 673601, India

played a beneficial role in LED process of a series of pentaphenylsilole molecules. Since then, an aggregation-induced emission (AIE) for non-fluorescent compounds and aggregation-induced emission enhancement (AIEE) for weakly fluorescent molecules have been a mainstream area of research as it solved the problem related to the harmful effect of ACQ. It had been postulated that the restriction of intramolecular motions of the compound in an aggregate state could be a strong reason for the AIE /AIEE process [13, 14]. The cyano group plays a crucial role in AIEE phenomenon and a lot of structural candidates were reported in this regard such as butterfly shaped 2-{2,6-Bis[4-(cholesteryloxymethyl)styryl]-4*H*-pyran-4-ylidene}malononitrile [15], tetraphenylethene based fumaronitrile [16], α-cyano stilbene derivatives [17], 2,3-dicyano-5,6-diphenylpyrazine (DCDPP) [18] etc. As far as our concerned awareness, first time it is reporting that a phthalonitrile based compound showing AIEE property in the UV region.

Fluorescein, rhodamine and structural analogues constitute an important class of fluorescent xanthene dyes [19]. Fluorescein has diverse applications on account of its distinctive spectroscopic properties [20] such as long absorption-emission wavelength in the visible region, high fluorescence quantum yield in aqueous media, large extinction co-efficient, and photostability. Fluorescein and its derivatives possess a wide spectrum of biological applications in cellular biology and medical diagnosis [21–23]. The spectroscopic and photophysical properties of fluorescein can be tuned by introducing electron releasing and withdrawing groups on to the periphery of xanthene unit [24, 25]. In recent days the rational development of selective and sensitive fluorescent probes capable of detecting heavy and transition metal ions have gained considerable attention [26]. Iron plays a pivotal role in vital systems as an essential trace element [27] as well as an important structural component and cofactor of biologically relevant systems [27, 28] such as haemoglobin, myoglobin, cytochromes, ferridoxin etc. Moreover, iron is a significant environmental and industrial pollutant and the selective recognition of Fe^{3+} by fluorescent probes from samples implies of great significance. Fluorescein and its structural analogue rhodamine have been widely used as ratiometric fluoroionophores due to their characteristic acid-spirolactam structure, which can 'open-close' with an 'on–off' fluorescence response [29, 30]. Usually, fluorescein based fluorescent probes exist in the closed spirolactam form, which are colourless and non-fluorescent, while the addition of metal ion with specific recognizable property opens the xanthene core by metal induced tuatomerism due to chelation and the fluorescence of xanthene dye get enhanced significantly [31]. A large number of fluorescein based metal chemo sensors were designed and developed based on the aforementioned principle. However, to the best of our knowledge, there are no reports on fluorescein based chemo sensor derivatives where the fluorescein always existed in the spirolactam form. In the present study, we are locking the two hydroxyl group fluorescein by ethereal linkage with phthalonitrile group which are expected to be having electron withdrawing effect due to the presence of cyano groups. As a result of this $^{max}\lambda_{abs}$ and $^{max}\lambda_{em}$ of fluorescein dye is hypsochromically switched on to the near UV region.

Experimental

Materials and Methods

All chemicals and solvents were commercially purchased and used as received. 4- Nitrophthalonitrile and fluorescein were purchased from Sigma Aldrich. UV-visible absorption spectra and fluorescence spectra were recorded on a Schimadzu UV-Visible 2600 Spectrophotometer and Cary Eclipse Fluorescence Spectrophotometer of Agilent Technologies respectively with quartz cuvette. FT-IR spectra (KBr pellets) were recorded on a JASCO FT-IR 4700 spectrometer from Dept. of Chemistry, NIT Calicut. ^{1}H NMR spectra were obtained in deuterated chloroform $CDCl_3$, using a BrukerAvance III, 400 MHz FT-NMR spectrometer with TMS as internal reference. The X-ray diffraction data were measured at room temperature (293 K) using a Bruker Kappa Apex II diffractometer, equipped a fine focus sealed tube using X Shell software.

Synthesis of 4,4′-(Fluoresceinoxy) Bisphthalonitrile FPN

4,4′-(fluoresceinoxy) bisphthalonitrile FPN was prepared by adopting the well documented literature procedure for base catalysed aromatic nucleophilic ipso-nitro substitution reactions [32, 33].Fluorescein (0.5 g, 1.505 mmol) and 4-nitrophthalonitrile (0.521 g, 3.011 mmol) were added successively with stirring to dry DMF (20 mL), which was dried over molecular sieves of dimension 4A°. After dissolution, anhydrous K_2CO_3(1.246 g, 9.033 mmol) in aliquots of regular intervals was added and the reaction mixture was stirred at 60 °C for 48 h under purged nitrogen. The progress of the reaction was monitored by TLC. The reaction mixture was poured into 250 mL of ice cold 10% HCl solution and stirred for 15 min. The precipitate was filtered, washed several times with cold water, 1% NaOH in order to remove excess co-reactant fluorescein and again with cold water solution until the filtrate became neutral. The crude was dried in vacuo. The crude was subjected to recrystallization from DCM-methanol mixture, bright yellow crystals of the pure product is obtained. Yield: 0.735 g (72%). The single crystals of the compound were developed from DCM-methanol mixture by solvent diffusion technique. The molecular structure of the compound with atom numbering scheme is represented in Fig. 1.

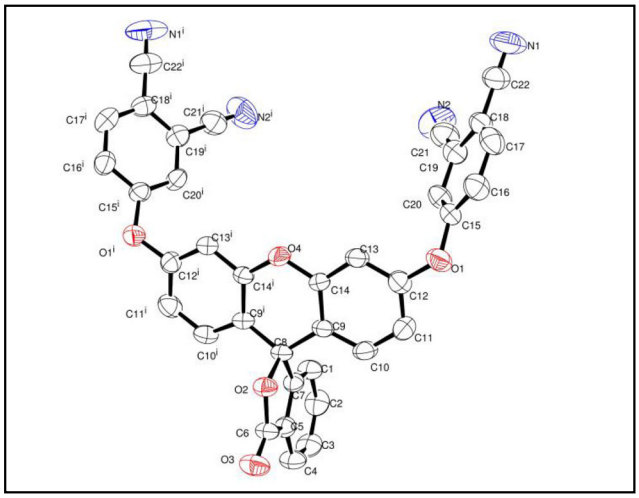

Fig. 1 ORTEP view of the molecular structure of FPN. Hydrogen atoms are omitted for clarity and the ellipsoids are drawn at 50% probability

UV–vis ($CHCl_3$): λ_{max}, nm (log ε): 345 (4.70); FTIR _ (cm − 1): 3060–3003 (Ar–CH), 2969–2837 (aliphatic –CH), 2232 (C N) 1716 (C=O lactone), 1583–1463 (C=C), 1292, 1267 (Ar–O–Ar), 1233–1118 (Ar–O–C).

^{1}HNMR ($CDCl_3$): Lactone ring protons A 8.1 (d, 1H, ^{3}J = 7.6), C 7.78 (t, 1 H, ^{3}J = 7.6 Hz), B 7.7 (t, 1H, ^{3}J = 7.6 Hz), D 7.29 (d, 1H, ^{3}J = 7.6 Hz) 7.26 Solvent peak $CDCl_3$ Phenyl ring protons 7.78 Taller peaks (d, 2H, J^3 = 8.6 Hz) triplet of lactone ring at 7.78 and this doublet combinatorial exist as a multiplet(m), 7.37 (s, 2H, ^{4}J = 2.2 Hz), 7.35 (dd, 2H, J^3 = 8.6 Hz, J^4 = 2.2 Hz), 7.03 (s, 2H, ^{4}J = 2.4 Hz), 6.94 (d, 2H, ^{3}J = 8.6 Hz), 6.81 (dd, 2H, (J^3 = 8.8 Hz, J^4 = 2.4 Hz).

Result and Discussion

Synthesis and Characterization Data

The compound 4,4′-(fluoresceinoxy) bisphthalonitrile FPN was synthesized by the general base catalysed coupling reaction adopted for the synthesis of modified phthalonitrile. The reaction involves the mechanism of base catalysed aromatic ipso nitro substitution of 4-nitrophthalonitrile with fluorescein in the presence of K_2CO_3 as base in DMF under a N_2 atmosphere at 60 °C. The reaction was carried out by taking the reactant 4-nitrophthalonitrile in 1 M and 2 M equivalent with respect to fluorescein as in trial and error basis. The newly synthesized compound FPN was well characterized by routine spectroscopic methods such as UV–vis., fluorescence, FT-IR, ^{1}H NMR and single crystal X-ray diffraction method. These characterization results, especially ^{1}H NMR and single crystal XRD data, invariably pointed out that the product of the base catalysed coupling reaction is always a 1:2 not 1:1 in the similar reaction conditions irrespective of the fact that the co-reactants fluorescein and 4-nitrophthalonitrile is taken in 1:1 or 1:2 stoichiometric ratio. The plausible reason for the formation of the product 4,4′-(fluoresceinoxy) bisphthalonitrile is that fluorescein can be able to exist in two tautomer structure such as open tautomer "acid" form as well as closed "spirolactam" form. Since the reaction was carried out in dipolar aprotic solvent DMF, "spirolactam" form predominates and the resultant product will be 1:2 stoichiometric product 4,4′-(fluoresceinoxy) bisphthalonitrile FPN as depicted in the Scheme 1.

The disappearance of broad O-H peak of fluorescein combined with aromatic C-H peak at 3078 cm^{-1} as well as the asymmetric and symmetric NO_2 stretching bands of 4-nitrophthalonitrile at 1539, 1356 cm^{-1} in the FT-IR spectra and the confirmed the formation of desired product FPN. (Fig. S2 in ESI). The ^{1}HNMR analysis performed in $CDCl_3$ solvent was in good agreement with the theoretically predicted structure of FPN and detailed spectral assignment is given in Fig. S3 and Table S2 of ESI. The compound FPN was successfully characterized by single crystal X-ray diffraction studies. The crystals were obtained by solvent diffusion crystallization technique from DCM-methanol mixture of the complex at room temperature. The detailed crystal data and parameters are given in Table S4 of ESI and the selected bond lengths and bond angles are given in Table S5 of ESI. The unit cell and the brief description of molecular packing diagram of FPN are given in Fig. S4 of ESI.

Fluorescence Quantum Yield and Solvatochromic Behavior of FPN

The optical properties of the compound FPN were investigated by UV-visible absorption and fluorescence emission spectroscopic studies in various solvents. A stock solution of FPN was prepared in fresh DMF at room temperature. The fluorescence quantum yield (Φ_F) of FPN was determined in organic solvents such as hexane, cyclohexane, THF, DCM, DMF, acetonitrile, ethanol and in methanol at room temperature by the comparative method [34, 35] using Eq. (1)

$$\Phi_F = \Phi_F(Std)\frac{F\,A_{Std}n^2}{F_{std}\,A\,n^2_{Std}} \quad (1)$$

where F and F_{Std} are the areas under the fluorescence emission curves of the compound FPN and standard respectively. A and A_{Std} are the respective absorbances of FPN and standard at the excitation wavelength 300 nm and n^2 and n^2_{Std} are the respective refractive indices of solvents used for the sample and standard, ie. organic solvents and 0.1 M H_2SO_4 respectively. Φ_F and Φ_F (Std) are the respective quantum yields of FPN and standard. 2-aminopyridine in 0.1 M H_2SO_4 (Φ_F = 0.60) was employed as the standard [36]. The absorbance of the sample FPN in different organic solvents and the standard 2-aminopyridine in 0.1 M H_2SO_4 was ranged below 0.08 at the excitation wavelength 300 nm.

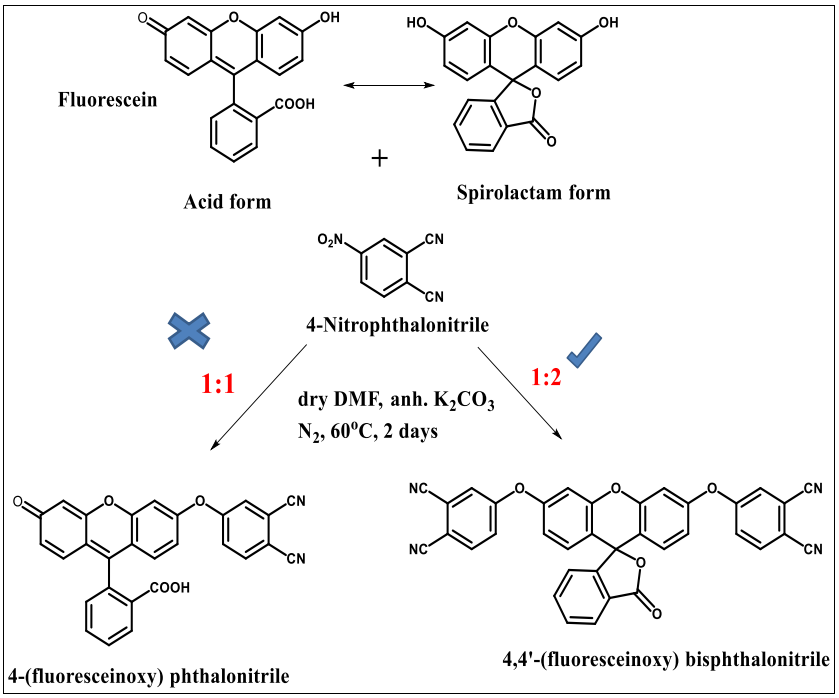

Scheme 1 Synthesis of 4,4′-(fluoresceinoxy) bisphthalonitrile FPN from fluorescein and 4-nitrophthalonitrile

The normalized absorption-emission spectra of FPN and solid state fluorescence spectra of FPN in the amorphous-crystalline states are displayed in Fig. 2a, b respectively. The major peaks in absorption spectrum in DMF were situated at 265, 295 and 305 nm, whereas the emission band of FPN was situated at 458 nm as shown in Fig. 2a (Stoke shift of 153 nm). The solid state emission spectra of FPN in the amorphous state shows $^{max}\lambda_{em}$ at 396 nm is shifted to 412 nm in crystalline state by a phase shift of 16 nm.

It is documented that the acceptor-donor–acceptor A-D-A systems connected by a bridging atom or a group, generally referred to as spacer, is well known to display solvatochromism [37]. Here the present case deals with the compound FPN which is formed by the electron donor D fluorescein unit sandwiching between two electron acceptor A phthalonitrile units by bridging oxygen atoms. Cyano group bearing compounds have been widely used as acceptors for light emitting chromophores [15–17, 38]. The solvatochromic study of FPN was performed by fluorescence spectra in various organic solvents of increasing order of polarity such as hexane, cyclohexane, THF, DCM, DMF, acetonitrile, ethanol and methanol with a constant concentration of FPN (1×10^{-5}M) as shown in Fig. 3. The photophysical quantum yield ΦF and molar extinction coefficient ε of FPN in different solvents arranged in the ascending order relative polarity is given in Table 1.

The compound FPN was found to be exhibiting positive solvatochromic behaviour i.e., as the polarity of solvents increases from hexane to methanol the emission band λ_{em} bathochromically shifted from 381 to 458 nm. This solvatochromic property is explained in terms of the Intramolecular Charge Transfer ICT process prevailed in A-D-A systems [39–41]. When the molecule is excited, ICT process happens from donor to acceptor which results in a

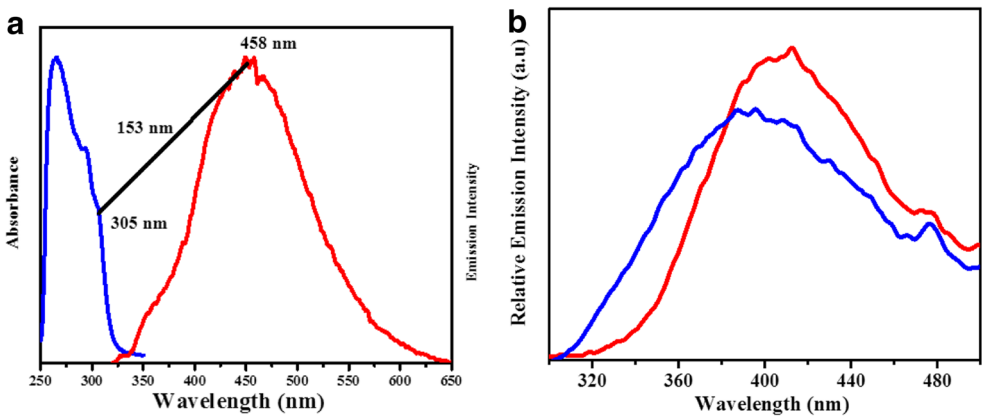

Fig. 2 **a** Absorption (blue) and emission (red) spectra of FPN in DMF and **b**. solid state fluorescence spectra of FPN in powder (blue) and in crystalline form (red)

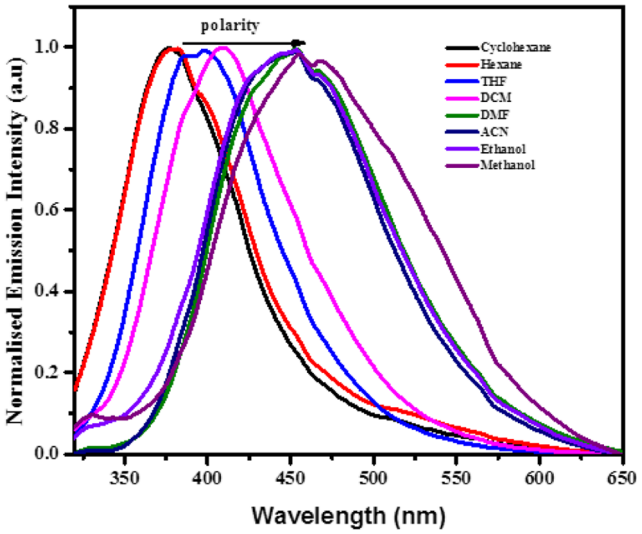

Fig. 3 Emission spectra of FPN of concentration (1×10^{-5}M) in cyclohexane, hexane, THF, DCM, DMF, acetonitrile, ethanol and in methanol ($\lambda_{ex} = 300$ nm)

dipole moment change and exhibit greater degree of electronic polarization. If the dipole moment of the excited state is greater than that of the ground state, so the solvent of increasing polarity can lower the energy of the excited state by solvation process prior to emission. Therefore the excited state is more stabilized in polar solvents compared to non-polar solvents, which in turn causes red shift and results in positive solvatochromism [42].

Aggregation Induced Emission Enhancement AIEE

Aggregation is described as the coplanar association of aromatic rings progressing from monomer to dimer and higher order structures, driven by nonbonded attractive interactions. Aggregation process perturbs the electronic structure of the compound resulting in alternation of the ground and excited state electronic structures [43]. The compound FPN was found to be very well soluble in common organic solvents such as THF, DCM, DMF and ACN. But polar protic solvents such as ethanol, methanol and water were found to be poor solvents for FPN. Usually, a good and poor solvent pair, where both the solvents are readily miscible is chosen for a compound to perform aggregation studies and the electronic spectrum gives a clear cut idea of aggregation from the deformed nature and broadness of the spectra. Here we have adopted the electronic absorption and fluorescence emission spectra of the compound to evaluate the aggregation tendency of FPN (stock prepared in DMF) in DMF-water mixture by varying the volume percentage of water from 0 to 98% under identical conditions at room temperature (Fig. 4a, b). AIEE experiment was carried out for fixed concentration of FPN in DMF by varying the volume percentage of water and DMF mixture from 0 to 98%. All the solutions are excited at 300 nm in a 1 cm path length fluorescence cuvette of 1 ml capacity with excitation and emission slit widths of 5 nm each.

Initially, as the percentage of water was increased from 0 to 50%, some slight decreases were observed in the absorbance of the electronic spectra, while the fluorescence intensity at identical conditions was found to be gradually decreased and leveled off to tail with a slight bathochromic shift, as that naturally seen in ACQ species. This can be explained in terms of both dilution and ACQ property of water [44]. But when the volume of water reached beyond 50%, the compound FPN exhibited severe aggregations (as evident from deformed and broadened peaks of UV-vis spectra) with an enormous increase in fluorescence intensity followed by a hypsochromic shift of 70 nm for the emission wavelength, i.e., from $\lambda_{em} =$ 458 to 388 nm (Fig. 4b and 5), an abnormal phenomenon

Table 1 Absorbance and emission characteristics of FPN in different solvents

Solvents	$^{Abs}\lambda_{max}$ (nm) with log ε	$^{em}\lambda_{max}$ (nm)	Refractive index (n)	Quantum yield (Φ_F)
Cyclohexane	N.D	376	1.427	0.046
Hexane	N.D	378	1.375	0.059
THF	245 (4.45) 293 (4.037) 304 (3.874)	393	1.407	0.088
DCM	236(4.484) 256(4.36) 294(3.91) 304(3.762)	410	1.424	0.124
DMF	271(4.35) 294(4.17) 305(4.02)	458	1.431	0.0087
ACN	251(4.47) 293(4.12) 303(3.96)	462	1.344	0.093
Ethanol	N.D	465	1.361	0.08
Methanol	N.D	468	1.331	0.055

N.D, Peaks are not detectable due to aggregation phenomenon

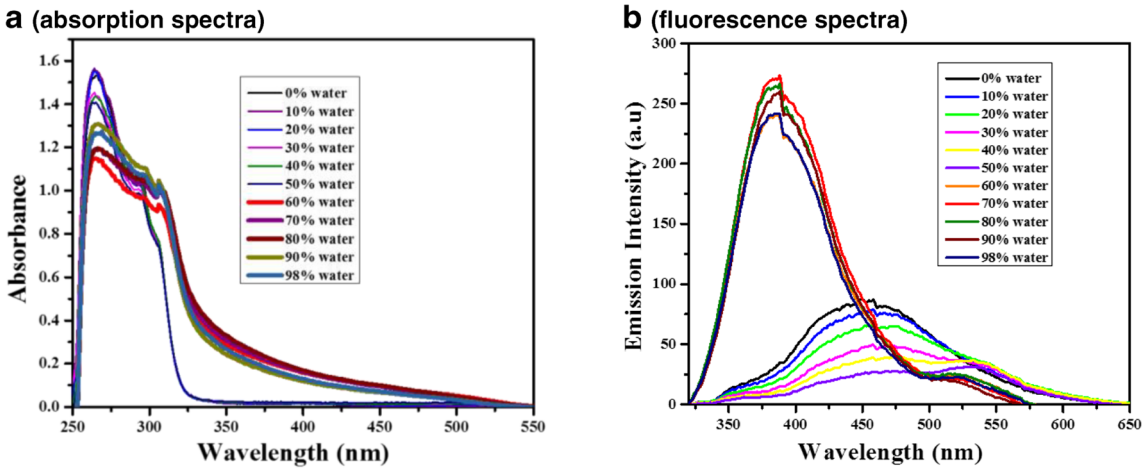

Fig. 4 Aggregation study of FPN: **a** UV-visible spectra and **b** fluorescence spectra of FPN of concentration (0.087 mM) in DMF-water mixture where volume (%) of water was increased from 0 to 98%

referred to as Aggregation Induced Blue Shifted Emission Enhancement, AIBSEE [45, 46], a special kind of AIEE. The fluorescence quantum yield of FPN in DMF is calculated as 0.0087, but with the addition water which is changed as 0.06 clearly indicated that AIEE phenomenon happened in the DMF-water mixture of FPN.

The compounds exhibiting AIEE behavior can be explained by scrutinizing the structural peculiarities of the molecule. The compound FPN can be considered to be a pull-push-pull acceptor-donor-acceptor (A-D-A) system connected by spacer atoms, where the fluorescein unit served as donor, with the two phthalonitrile units as acceptor, which are linked together by heteroatom O as spacer [47]. The fluorescence intensity of FPN was lesser compared with the parent fluorescein moiety in the open quinoid form, however, its emission was significant compared to that of fluorescein in the closed spirolactam form. The fluorescence of FPN originates due to the electron withdrawing effect of phthalonitrile subunits through the spacer atom O by the process of Intramolecular Charge Transfer, ICT. But the counteracting process which decreases the fluorescence intensity of FPN was the single bond free rotation or dynamic intramolecular rotation of phthalonitrile units about the O atom, which causes a non-radiative decay [48]. As per the crystallographic data, FPN molecule is having a non-planar conformation in the ground state, i.e. xanthene unit of fluorescein and two phthalonitrile units of FPN stay in different planes, so ground state of FPN in DMF showing blue fluorescence prior to water addition. But with the gradual introduction of water from 0 to 50% the fluorescence intensity of FPN gradually decreased and levelled off to tail in conjunction with a bathochromic shift. This fluorescence quenching may be related to the intensive hydrogen bond interactions around the monomers of FPN and

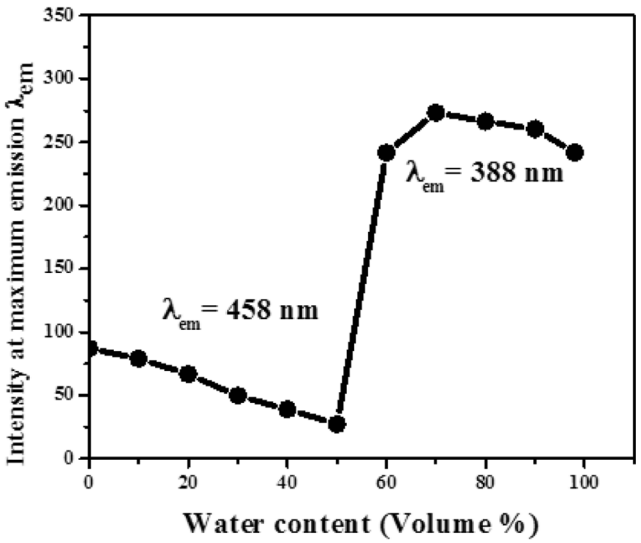

Fig. 5 Graphical representation of AIEE of FPN in DMF-water mixture in which the volume of water increased from 0 to 98%

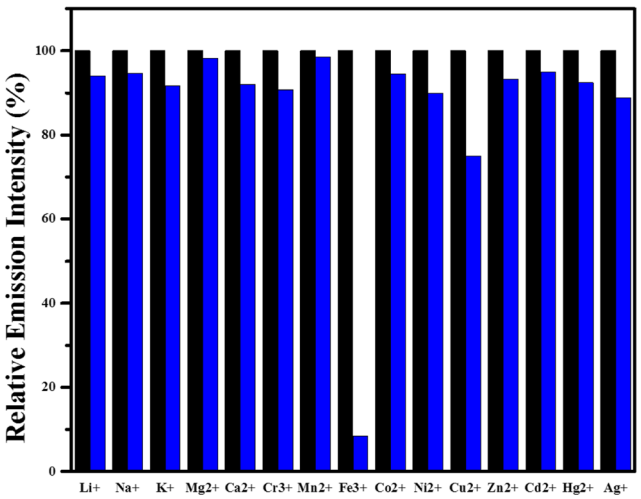

Fig. 6 Fluorescence responses of FPN at 419 nm in the presence of different metal ions: Li^+, Na^+, K^+, Mg^{2+}, Ca^{2+}, Cr^{3+}, Mn^{2+}, Fe^{3+}, Co^{2+}, Ni^{2+}, Cu^{2+}, Zn^{2+}, Cd^{2+}, Hg^{2+} and Ag^+ (as their chloride salts, except $MgSO_4$ and $AgNO_3$) in ACN/methanol (9:1 *v*/v). [FPN] = 0.5 mM, [Mn+] = 5 mM. Ratio of [FPN]:[Mn+] = 1:10

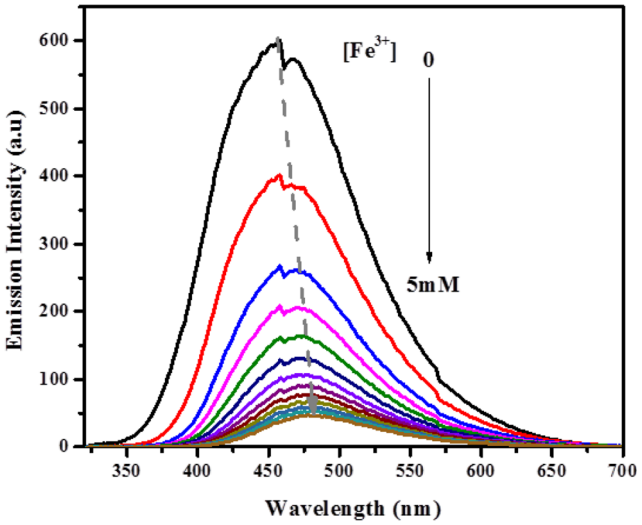

Fig. 7 Emission spectra of FPN (0.5 mM) in acetonitrile ACN-methanol (*v*/v = 9:1) mixture upon the addition of 0–5 mM of Fe^{3+} in methanol as 500 μM increment. The excitation wavelength was 300 nm

the longer wavelength shift arises by the stabilization of locally excited LE state, which is generated by ICT of twisted FPN, in more polar DMF-water mixture [49]. The microscopic structural characterization of the aggregated species is difficult and hence the underlying mechanism of AIBSEE still remains unclear [50]. However, it was speculated that Restricted Intramolecular Rotation (RIR) and suppression of Twisted Intramolecular Charge Transfer (TICT) is the plausible reason for AIEE with concomitant blue shift known as AIBSEE. The aggregation force become predominant over other factors, as the fraction of water reaches greater than 50%. Therefore when FPN molecule is excited the non-planar geometry of FPN assumes a aggregation induced locally excited LE state characterized by strained planar conformation of low dipole moment in the highly aggregated state and this LE state is destabilized by the highly polar DMF-aqueous mixture [51]. So the energy gap between excited state and ground state becomes increases, which results in hypsochromic shift. In addition to this, the free rotation about the freely single O bridge bond is hindered on account of severe aggregation. Thus RIR and suppression of TICT is the plausible reason for AIEE with concomitant blue shift known as AIBSEE.

Chemo Sensing Study

As a fluorescent compound with cyano functional groups capable of interaction with metal ions, the chemo sensing property of FPN was quite interesting to be investigated. Hence in the current work, we have also performed a sensing study of FPN towards various transition as well as non- transition metal ions by emission spectroscopy. In order to evaluate the selectivity and sensitivity of FPN towards metal cations, fluorescence spectra of FPN was measured in the presence of various cations i.e., Li^+, Na^+, K^+, Mg^{2+}, Ca^{2+}, Cr^{3+}, Mn^{2+}, Fe^{3+}, Co^{2+}, Ni^{2+}, Cu^{2+}, Zn^{2+}, Cd^{2+}, Hg^{2+} and Ag^+. The changes in the fluorescence spectral intensity of FPN with the addition of double the molar concentration of each metal ion were measured and the relative intensity changes were represented in bar diagrams as given in Fig. 6. As a uniform procedure, chloride salts of the metals were taken for the study, except in the cases of $AgNO_3$ and $MgSO_4$. The fluorescence spectra of FPN exhibited insignificant quenching (≤10%) towards most of the metals added except for Fe^{3+} ion, in which the relative emission intensity was reduced by 91.35%.

The fluorescence titration of FPN against Fe^{3+} was carried out by taking FPN and Fe^{3+} in 1:10 M ratio. A stock solution of FPN was prepared in acetonitrile, which is chosen as an appropriate solvent of ΦF is 0.093. The blank emission spectra of FPN were run in pure ACN for ten times for standard deviation to calculate the limit of detection (LOD). A fixed volume increment of FeCl3 in methanol was added stepwise where the spectral changes for each addition were noted, till the concentration of FPN and Fe^{3+} reached a 1:10 ratio. An enormous decrease in the emission intensity (more than 50%) of FPN was noted with the addition of first increment of Fe^{3+}, which was leveled off to tail at the end of titration (Fig. 7). The extent of quenching was quite low in water media (Fig. S5 in ESI) compared to that in organic solvents, most probably due to the counteracting AIEE phenomenon.

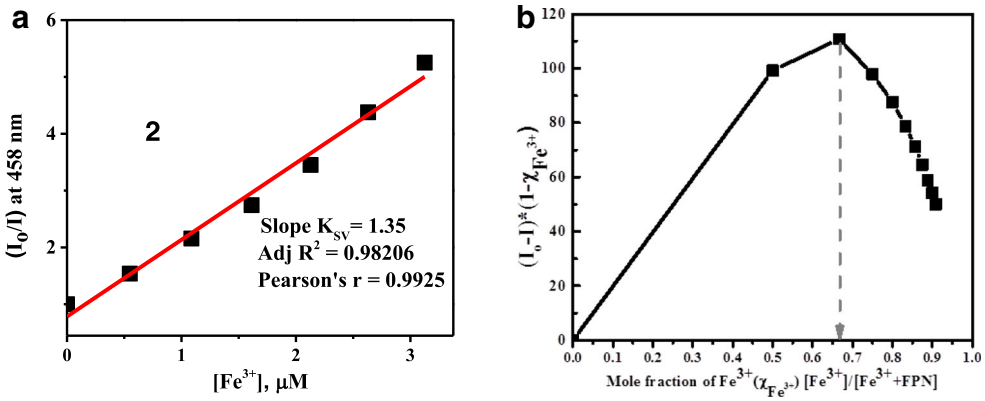

Fig. 8 **a**. Stern-Volmer emission profile of FPN with the addition of Fe^{3+} to calculate LOD and **b** Jobs plot showing the variation of fluorescence intensity against mole fraction of Fe^{3+}

Table 2 Comparison with the LOD values of literature reported Fe^{3+} fluorescence turn off chemosensor

SI No.	Compound name	Structure	LOD (mol/L)	Year	References
1	polyacrylamide covalently linked to N-acryl-N″-(rhodamine B-yl) diethylenetriamine **(poly(AM–ARBD))**	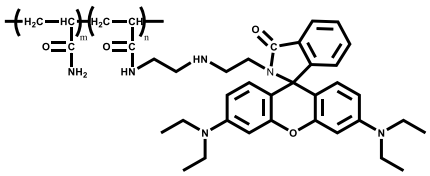	1.34×10^{-4}	2014	[55]
2	(E)-3-((3,4-dihydroxybenzylidene)amino)-7-hydroxy-2H-chromen-2-one **BS1**	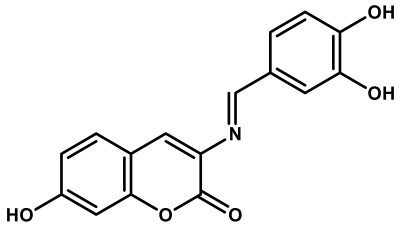 **BS1**	5.17×10^{-5}	2014	[56]
	(E)-3-((2,4-dihydroxybenzylidene)amino)-7-hydroxy-2H-chromen-2-one **BS2**	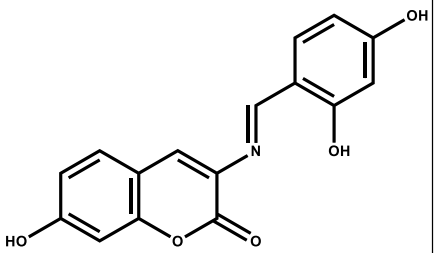 **BS2**	4.87×10^{-5}		
3	(E)-2-((4-(diphenylamino) benzylidene)amino)phenol **S1**	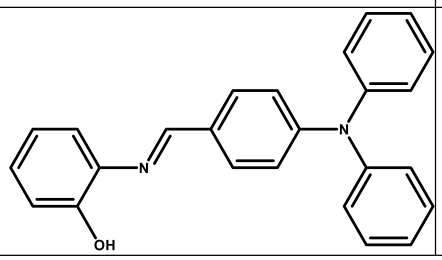	4.51×10^{-5}	2017	[57]

From Stern-Volmer emission spectral profile with the addition of Fe^{3+} given in Fig. 8a, the limit of detection, LOD of the chemosensor FPN for Fe^{3+} was determined using the eq. (2) [52–54].

$$\mathrm{LOD} = \frac{\mathbf{3} \times \boldsymbol{STD}}{\boldsymbol{S}} \tag{2}$$

where STD is the standard deviation of the blank solution of FPN and S is the slope of the Stern-Volmer calibration curve and the LOD value was found to be 3.665 μM and it is corrected as 3.665 ± 0.016 by including the error of the triplicated experiment. This result pointed out that the chemo sensor FPN is highly efficient in sensing Fe^{3+} ion even in the minute level concentration equal to or greater than

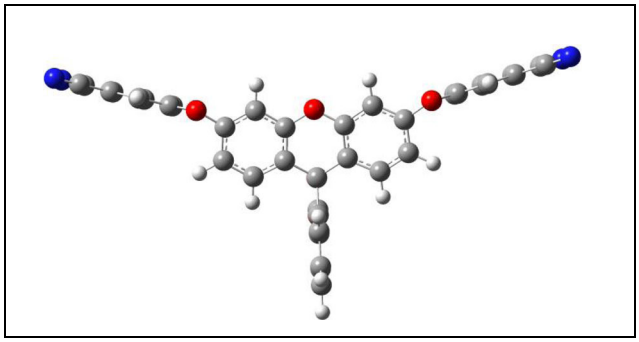

Fig. 9 Optimized structure of FPN

3.665 μM. In Table 2 we compared the LOD value of FPN with other literature reported Fe^{3+} turn off fluorescent chemosensors. Therefore we can recommended that FPN is a potential chemo sensor candidate for the selective detection of Fe^{3+} ion by fluorescence turn off mechanism with fairly good LOD value.

The Job's plot method was used to get an insight into the binding stoichiometry of chemosensor FPN-Fe^{3+} complexes. In Fig. 8b, the mole fraction of analyte Fe^{3+}, $\chi_{Fe}{}^{3+}$ against the emission intensity factor (Io-I)(1- $\chi_{Fe}{}^{3+}$) at 462 nm was plotted and the apex of the V-shaped graph corresponded to 0.667. The result indicated that binding stoichiometry of FPN with Fe^{3+} was 1:2, ie two Fe^{3+} atoms bound to a single molecule of FPN [58].

Computational Methodology

Among the different computational tools available, the Density Functional Theory (DFT) has been used here because of its large accuracy and high predicting power of physical and chemical properties [59, 60]. The level of theory adopted was B3LYP, which consists of Becke's exchange functional [61] in conjunction with Lee-Yang –Parr correlational functional [62] and the basis set used is 6–31 + G (d, p) for FPN and Lanl2Dz for Fe^{3+} ion. All the computational works have been carried out through Gaussian 09 software package [63] with DFT-B3LYP as level of theory and the visualizations are done through the Gaussview-5.0 graphical user interface [64].

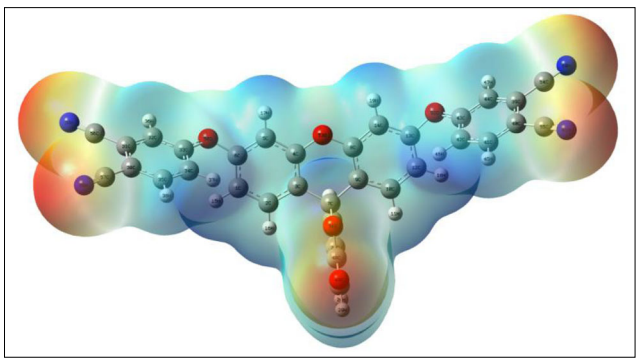

Fig. 10 ESP map of FPN

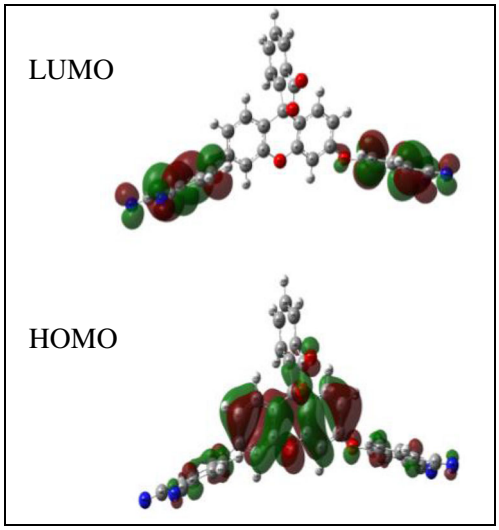

Fig. 11 HOMO-LUMO diagram of FPN

The molecular structure of FPN has been optimized by DFT-B3LYP/6–31+ G (d, p) and is shown in Fig. 9. It is not a planar molecule as shown in Fig. 9.

In order to find the nucleophilic and electrophilic regions in FPN, the Electrostatic Potential (ESP) map has been drawn and is shown in Fig. 10. the red color in ESP map shows the electron rich (nucleophilic) region while blue shows the electron deficient (electrophilic) region. Here, in the case of FPN, the elctron rich regions are located on oxygen and nitrogen atoms so that they are susceptible to electrophilic attack. Thus, the sensing of iron by FPN may be attributted to the presence of these nucleophilic sites in FPN and the cyano groups may take part in chelation with iron.

The chemical reactivity of every molecule has a dependence on the energy gap between their Highest Occupied Molecular Orbital (HOMO) and Lowest Unoccupied Molecular Orbital (LUMO). The HOMO-LUMO diagram of FPN has been shown in Fig. 11., clearly shows that the LUMO of FPN has been delocalized over the two phthalonitrile rings and iron while the HOMO has been delocalized over the xanthine system and partially on the lactone ring. The energy gap of FPN is found to be 4.53 eV. The delocalization of LUMO over the two phthalonitrile rings and iron indicates that there some interaction between the EPN and metal ion and this may be due to some charge transfer which results in quenching of fluorescence.

The fluorescence of FPN (low as compared to the inherent quantum yield of fluorescein in acid form but high as in the spirolactam form) is likely to happen by ICT process in fluorescein by phthalonitrile units. Therefore in FPN the –CN groups are nucleophilic so that it have some affinity towards metal ions. Here based on the results of fluorescence titration experiments, we proposed plausible binding modes for FPN + Fe^{3+} computationally for the fluorescence quenching of FPN with the addition of Fe^{3+}. Fe^{3+} is paramagnetic with

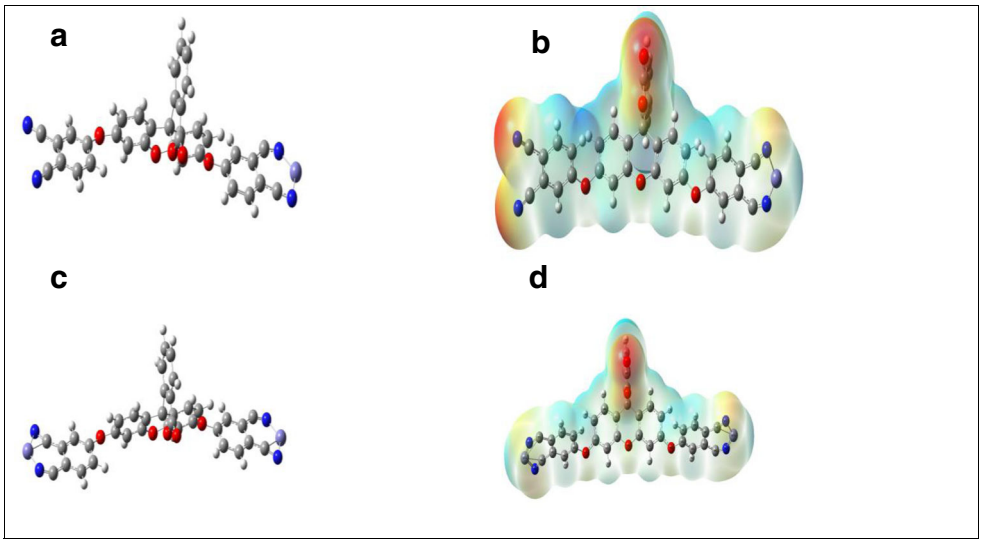

Fig. 12 **a** Optimized structure of 1:1 FPN-Fe complex, **b** ESP of 1:1 FPN-Fe complex, **c** Optimized structure of 1:2 FPN-Fe complex, **d** ESP of 1:2 FPN-Fe complex

5 unpaired d shell electrons and could strongly quench the emission of fluorophore to the proximity through electron and/or energy transfer processes. The cyano groups on FPN binds with Fe^{3+} ion and forming 1:1 and 1:2 FPN-Fe complexes (see Fig. 12a, c). The stabilization energy (E_{sta}) for 1:1 and 1:2 complexes obtained by the difference in energies of FEN, Fe^{3+} ion and FPN-Fe complexes are negative so that they are highly stable (see Table 3). The ESP map of FPN has red color on the nitrogen atom, indicating its nucleophilicity. This is decreased on complexation with Fe^{3+} shows that there is some charge transfer between FPN and the Fe^{3+} ion. This is clear from the ESP map of both 1:1 and 1:2 FPN-Fe complexes shown in Fig. 12b, d.

The fluorescence of FPN has been found to be quenched on complexation with Fe^{3+} ion. In order to evaluate this theoretically, the optimized structure of FPN has been subjected to complexation with Fe^{3+} ion. The final structure obtained (see Fig. 12a) shows that there is interaction between the ligand (FPN) and the Fe^{3+} ion. The HOMO-LUMO diagram of FPN-Fe complexes have shown in Fig. 13.

It has been observed that the band gap is decreased from 4.53 to 2.32 eV for 1:1 and 2.28 for 1:2 FPN-Fe complexes. Moreover, the HOMO of complex increases than that of ligand. When an electron from the HOMO of FPN excited to its LUMO and it return back to the HOMO again, to restore the ground state, results in fluorescence. The HOMO of FPN-Fe complex is found to be higher than that of FPN, but lower than the LUMO of FPN, i.e., the HOMO of FPN-Fe complex lies in between the HOMO and LUMO of FPN. The HOMO of complex has been delocalized on the phthalonitrile group with Fe^{3+} ion. So in presence of Fe^{3+} ion, the complexation takes place and its HOMO donates electron to the HOMO of FPN and converts it into its ground state resulting in the quenching of fluorescence (see Fig. 14) [65–68]. In both 1:1 and 1:2 FPN-Fe complexes, the HOMO lies in between the HOMO and LUMO of FPN. So quenching has been seen in both cases. The experimental result obtained from Job's plot analysis revealed that the compound FPN interacts with Fe^{3+} in a 1:2 stoichiometric ratio. The experimental result is in good agreement with the computational modelling observations, in which the stabilization energy (E_{sta}) is higher for 1:2 complexes than 1:1 complexes.

Conclusions

We have studied the positive solvatochromic behaviour of the newly synthesized 4,4′-fluoresceinoxy bisphthalonitrile, FPN in various organic solvents of increasing polarity such as cyclohexane, hexane, THF, DCM, DMF, acetonitrile, ethanol and methanol by fluorescence spectroscopy. The aggregation tendency of the compound FPN was investigated in DMF-aqueous mixture,

Table 3 Thermo-chemical parameters of the complexes

Complex	E_{sta} (HF)	Dipole moment (Debye)	Entropy (cal/mol)	Enthalpy (HF)	Free energy (HF)	ΔE (eV)
1:1	−244.398	9.41	233	−2099.05	−2099.16	2.32
1:2	−367.727	5.70	237	−2222.38	−2222.49	2.28

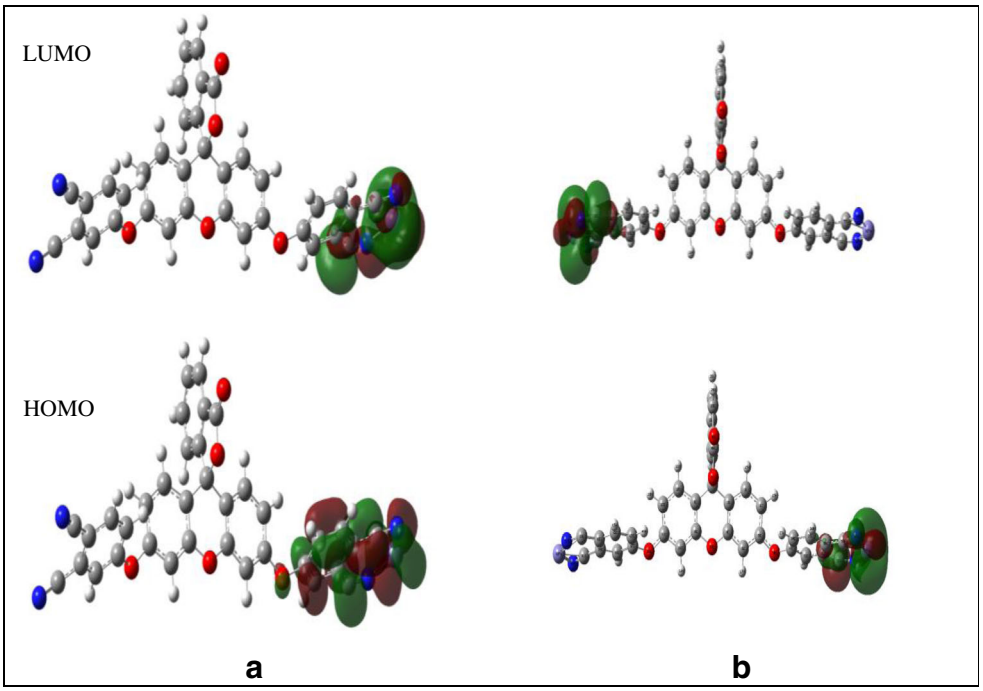

Fig. 13 HOMO-LUMO diagram of (**a**) 1:1 FPN-Fe complex, (**b**) 1:2 FPN-Fe complex

where it was found to be exhibiting AIEE property. As the volume of water exceeded beyond 50%, a hypsochromic shift of 70 nm was observed for λ_{em} from 458 to 388 nm, which is known as Aggregation Induced Blue Shifted Emission Enhancement, AIBSEE. This property can be explained on the basis of the Acceptor-Donor-Acceptor structural constitution of FPN, restricted intramolecular rotation (RIR) and twisted intramolecular charge transfer (TICT) processes and the formation of locally excited (LE) state of the molecule in the aggregated state. In addition to the aggregation study, chemo sensing behaviour of FPN was also checked towards various transition metal ions in ACN:MeOH (9:1 *v*/v) mixture, where the molecule FPN has selectively exhibited a fluorescence turn off behaviour towards Fe^{3+} ion with a LOD value of 14.49 μM. Job's plot analysis suggested that FPN binds with Fe^{3+} in 1:2 stoichiometric ratio where the two phthalonitrile units of one FPN unit bind with two Fe^{3+} ions. The computational studies pointed out that FPN could interact with Fe^{3+} both in 1:1 and 1:2 ratio as the HOMO of FPN-Fe complexes lies in range of the HOMO-LUMO gap of FPN. But the stabilization energy values of FPN-Fe complex invariably support the experimental observation, as E_{sta}(HF) of FPN-Fe complex in the 1:2 ratio is more negative than that in the case of 1:1 complex, so that the former one is more energetically favoured.

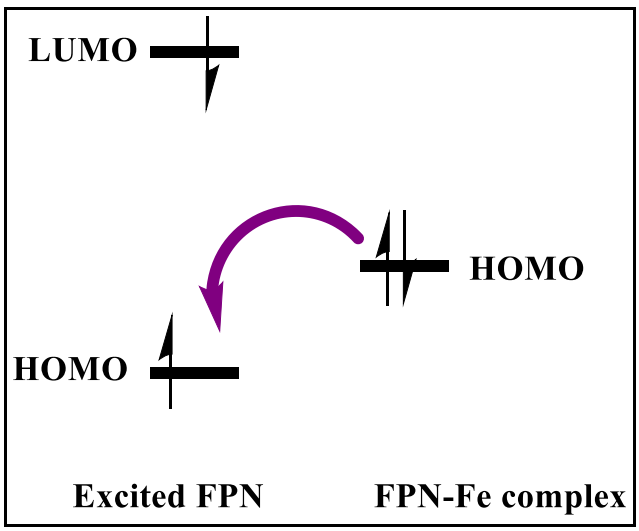

Fig. 14 Quenching of fluorescence

Acknowledgements Amitha G S is thankful to NCB-GATE for research fellowship and Suni Vasudevan would like to thank SERB – Dept. of Science and Technology (Grant Sanction No. SERB/F/3600/2013-14) for financial support. The co-author Vijisha K. Rajan expresses sincere gratitude to UGC for the financial support and Central Sophisticated Instrumentation Facility (CSIF) of University of Calicut for the Gaussian 09 software support. The authors would like to acknowledge Sophisticated Test Instrumentation Centre (STIC) of Cochin University of Science and Technology (CUSAT) for providing single crystal XRD facility. The Crystallographic Information File (CIF) of single crystal of FPN was deposited in Cambridge Crystallographic Data Centre with CCDC No. 1828283.

Compliance with Ethical Standards

Conflict of Interest The authors declare no conflict of interest.

Publisher's Note Springer Nature remains neutral with regard to jurisdictional claims in published maps and institutional affiliations.

References

1. MacCormac A, O'Brien E, O'Kennedy R (2010) Classroom activity connections: lessons from fluorescence. J Chem Educ 87:685–686. https://doi.org/10.1021/ed100262t
2. Blitz JP, Sheeran DJ, Becker TL, Danielson ND (2006) Classroom demonstrations of concepts in molecular fluorescence. J Chem Educ 83:758. https://doi.org/10.1021/ed083p758
3. Özçeşmeci I, Tekin A, Gül A (2014) Synthesis and aggregation behavior of zinc phthalocyanines substituted with bulky naphthoxy and phenylazonaphthoxy groups: An experimental and theoretical study. Synth Met 189:100–110. https://doi.org/10.1016/j.synthmet.2014.01.003
4. Hua F, Ruckenstein E (2004) Fluorescence study of aggregation in water of PEO-grafted polydiphenylamine. Langmuir 20:3954–3961. https://doi.org/10.1021/la036124h
5. Forster KK (1954) Konzentrationsabhängigkeit Fluoreszenzspek-. Z Phys Chem 1:275
6. Birks JB (1970) Photophysics of aromatic molecules. Wiley-Interscience, London
7. Zhang L, Liang K, Dong L, Yang P, Li Y, Feng X, Zhi J, Shi J, Tong B, Dong Y (2017) Aggregation-induced emission enhancement and aggregation-induced circular dichroism of chiral pentaphenylpyrrole derivatives and their helical self-assembly. New J Chem 41:8877–8884. https://doi.org/10.1039/C7NJ00583K
8. Venkatramaiah N, Kumar GD, Chandrasekaran Y, Ganduri R, Patil S (2018) Efficient blue and yellow organic light-emitting diodes enabled by aggregation-induced emission. ACS Appl Mater Interfaces 10:3838–3847. https://doi.org/10.1021/acsami.7b11025
9. Ong KH, Liu B (2017) Applications of fluorogens with rotor structures in solar cells. Molecules 22. https://doi.org/10.3390/molecules22060897
10. Ma H, Yang M, Zhang C, Ma Y, Qin Y, Lei Z, Chang L, Lei L, Wang T, Yang Y (2017) Aggregation-induced emission (AIE)-active fluorescent probes with multiple binding sites toward ATP sensing and live cell imaging. J Mater Chem B 5:8525–8531. https://doi.org/10.1039/c7tb02399e
11. Luo J, Xie Z, Lam JWY, Cheng L, Tang BZ, Chen H, Qiu C, Kwok HS, Zhan X, Liu Y, Zhu D (2001) Aggregation-induced emission of 1-methyl-1,2,3,4,5-pentaphenylsilole. Chem Commun 381:1740–1741. https://doi.org/10.1039/b105159h
12. An B, Kwon S, Jung S, Park SY (2002) Enhanced emission and its switching in fluorescent organic nanoparticles. J Am Chem Soc 124:14410–14415. https://doi.org/10.1021/JA0269082
13. Mei J, Hong Y, Lam JWY, Qin A, Tang Y, Tang BZ (2014) Aggregation-induced emission: the whole is more brilliant than the parts. Adv Mater 26:5429–5479. https://doi.org/10.1002/adma.201401356
14. Wang H, Zhao E, Lam JWY, Tang BZ (2015) AIE luminogens: emission brightened by aggregation. Mater Today 18:365–377. https://doi.org/10.1016/j.mattod.2015.03.004
15. Tong H, Hong Y, Dong Y, Ren Y, Häussler M, Lam JWY, Wong KS, Tang BZ (2007) Color-tunable, aggregation-induced emission of a butterfly-shaped molecule comprising a pyran skeleton and two cholesteryl wings. J Phys Chem B 111:2000–2007. https://doi.org/10.1021/jp067374k
16. Shen XY, Wang YJ, Zhao E, Yuan WZ, Liu Y, Lu P, Qin A, Ma Y, Sun JZ, Tang BZ (2013) Effects of substitution with donor-acceptor groups on the properties of tetraphenylethene trimer: aggregation-induced emission, solvatochromism, and mechanochromism. J Phys Chem C 117:7334–7347. https://doi.org/10.1021/jp311360p
17. Palakollu V, Kanvah S (2014) α-Cyanostilbene based fluorophores: aggregation-induced enhanced emission, solvatochromism and the pH effect. New J Chem 38:5736–5746. https://doi.org/10.1039/C4NJ01103A
18. Qin A, Lam JWY, Mahtab F, Jim CKW, Tang L, Sun J, Sung HHY, Williams ID, Tang BZ (2009) Pyrazine luminogens with "free" and "locked" phenyl rings: understanding of restriction of intramolecular rotation as a cause for aggregation-induced emission. Appl Phys Lett 94:2007–2010. https://doi.org/10.1063/1.3137166
19. de Meijere A (2005) Adolf von Baeyer: winner of the Nobel prize for chemistry 1905. Angew Chemie Int Ed 44:7836–7840. https://doi.org/10.1002/anie.200503351
20. Song A, Zhang J, Zhang M, Shen T, Tang J' (2000) Spectral properties and structure of fluorescein and its alkyl derivatives in micelles. Colloids Surfaces A Physicochem Eng Asp 167:253–262. https://doi.org/10.1016/S0927-7757(99)00313-1
21. Jampol LM, Cunha-Vaz J (1984) Diagnostic Agents in Ophthalmology: Sodium Fluorescein and Other Dyes. Springer, Berlin, Heidelberg, pp 699–714
22. Kanade S, Nataraj G, Ubale M, Mehta P (2016) Fluorescein diacetate vital staining for detecting viability of acid-fast bacilli in patients on antituberculosis treatment. Int J Mycobacteriology 5:294–298. https://doi.org/10.1016/j.ijmyco.2016.06.003
23. Grimm JB, Sung AJ, Legant WR, Hulamm P, Matlosz SM, Betzig E, Lavis LD (2013) Carbo fl uoresceins and Carborhodamines as Sca ff olds for high- contrast Fluorogenic probes. ACS Chem Biol 8:1303–1310. https://doi.org/10.1021/cb4000822
24. Kitley WR, Santa Maria PJ, Cloyd RA, Wysocki LM (2015) Synthesis of high contrast fluorescein-diethers for rapid bench-top sensing of palladium. Chem Commun 51:8520–8523. https://doi.org/10.1039/c5cc02192h
25. Feng S, Liu D, Feng W, Feng G (2017) Allyl fluorescein ethers as promising fluorescent probes for carbon monoxide imaging in living cells. Anal Chem 89:3754–3760. https://doi.org/10.1021/acs.analchem.7b00135
26. Jeong Y, Yoon J (2012) Recent progress on fluorescent chemosensors for metal ions. Inorganica Chim Acta 381:2–14. https://doi.org/10.1016/j.ica.2011.09.011
27. Kobayashi T, Nishizawa NK (2014) Iron sensors and signals in response to iron deficiency. Plant Sci 224:36–43. https://doi.org/10.1016/j.plantsci.2014.04.002
28. Brugnara C (2003) Iron deficiency and erythropoiesis: new diagnostic approaches. Clin Chem 49:1573–1578. https://doi.org/10.1373/49.10.1573
29. Chemate S, Sekar N (2015) A new rhodamine based OFF-ON fluorescent chemosensors for selective detection of Hg2+and Al3+in aqueous media. Sensors Actuators B Chem 220:1196–1204. https://doi.org/10.1016/j.snb.2015.06.061
30. An J, Yan M, Yang Z, Li TR, Zhou QX (2013) Dyes and pigments a turn-on fl uorescent sensor for Zn (II) based on fl uorescein-coumarin conjugate. Dyes Pigments 99:1–5. https://doi.org/10.1016/j.dyepig.2013.04.018
31. Venkatesan P, Thirumalivasan N, Wu S (2017) RSC advances a rhodamine-based chemosensor with diphenylselenium for highly selective fl uorescence. RSC Adv 7:21733–21739. https://doi.org/10.1039/C7RA02459B
32. Durmu M, Nyokong T (2007) Synthesis, photophysical and photochemical studies of new water-soluble indium(iii) phthalocyanines. Photochem Photobiol Sci 6:659. https://doi.org/10.1039/b618478b
33. Köysal Y, Şamil I, Akdemir N, Erbil A, McKee V (2003) 4-(8-Quinolinoxy)phthalonitrile. Acta Crystallogr Sect E Struct Reports Online 59:o1423–o1424. https://doi.org/10.1107/S1600536803018841
34. Ogunsipe A, Nyokong T (2005) Effects of central metal on the photophysical and photo- chemical properties of non-transition metal sulfophthalo- cyanine. 121–129
35. Sen P, Atmaca GY, Erdo muş A et al (2015) The synthesis, characterization, crystal structure and photophysical properties of a new meso-BODIPY substituted phthalonitrile. J Fluoresc 25:1225–1234. https://doi.org/10.1007/s10895-015-1609-y

36. Rusakowicz R, Testa AC (1968) 2-Aminopyridine as a standard for low-wavelength spectrofluorimetry. J Phys Chem 72:2680–2681. https://doi.org/10.1021/j100853a084
37. Dumur F, Gautier N, Gallego-Planas N, Şahin Y, Levillain E, Mercier N, Hudhomme P, Masino M, Girlando A, Lloveras V, Vidal-Gancedo J, Veciana J, Rovira C (2004) Novel fused D-A dyad and A-D-A triad incorporating Tetrathiafulvalene and p-benzoquinone. J Org Chem 69:2164–2177. https://doi.org/10.1021/jo035689f
38. Heiner Detert VS (2004) No TitleQuadrupolar donor–acceptor substituted oligo(phenylenevinylene)s—synthesis and solvatochromism of the fluorescence. J Phys Org Chem 17:1051–1056
39. Wen P, Gao Z, Zhang R, Li A, Zhang F, Li J, Xie J, Wu Y, Wu M, Guo KP (2017) A-π-D-π-a carbazole derivatives with remarkable solvatochromism and mechanoreponsive luminescence turn-on. J Mater Chem C 5:6136–6143. https://doi.org/10.1039/c7tc00559h
40. Sengupta S, Pandey UK (2018) Dual emissive bodipy-benzodithiophene-bodipy TICT triad with a remarkable stokes shift of 194 nm. Org Biomol Chem 16:2033–2038. https://doi.org/10.1039/c8ob00272j
41. Aydemir M, Haykir G, Türksoy F et al (2015) Synthesis and investigation of intra-molecular charge transfer state properties of novel donor-acceptor-donor pyridine derivatives: the effects of temperature and environment on molecular configurations and the origin of delayed fluorescence. Phys Chem Chem Phys 17:25572–25582. https://doi.org/10.1039/c5cp03937a
42. Lakowicz JR (2006) Principles of Fluorescence Spectroscopy. In: 3rd ed. Springer, Baltimore, US
43. Ben Zhong Tang AQ (2013) Aggregation-Induced Emission: Fundamentals and Applications, 1st ed. Wiley, Ltd
44. Li Q, Qian Y (2016) Aggregation-induced emission enhancement and cell imaging of a novel (carbazol-: N -yl)triphenylamine-BODIPY. New J Chem 40:7095–7101. https://doi.org/10.1039/c6nj01495j
45. Han X, Zhang B, Chen J, Liu SH, Tan C, Liu H, Lang MJ, Tan Y, Liu X, Yin J (2017) Modulating aggregation-induced emission via a non-conjugated linkage of fluorophores to. J Mater Chem B 5:5096–5100. https://doi.org/10.1039/C7TB00623C
46. Mazumdar P, Das D, Sahoo P, et al (2015) Exceptionally large blue shift and its potential. 3343–3354. https://doi.org/10.1039/C4CP03772C
47. Gopikrishna P, Raman Adil L, Iyer PK (2017) Bridge-driven aggregation control in dibenzofulvene–naphthalimide based donor–bridge–acceptor systems: enabling fluorescence enhancement, blue to red emission and solvatochromism. Mater Chem Front 1:2590–2598. https://doi.org/10.1039/C7QM00357A
48. Usuki T, Shimada M, Yamanoi Y, Ohto T, Tada H, Kasai H, Nishibori E, Nishihara H (2018) Aggregation-induced emission enhancement from Disilane-bridged donor-acceptor-donor Luminogens based on the Triarylamine functionality. ACS Appl Mater Interfaces 10:12164–12172. https://doi.org/10.1021/acsami.7b14802
49. Liu X, Qiao Q, Tian W, Liu W, Chen J, Lang MJ, Xu Z (2016) Aziridinyl fluorophores demonstrate bright fluorescence and superior Photostability by effectively inhibiting twisted intramolecular charge transfer. J Am Chem Soc 138:6960–6963. https://doi.org/10.1021/jacs.6b03924
50. Wu Q, Zhang T, Peng Q, Shuai Z (2014) Molecular picture from a QM / MM study. Photochem Photobiol Sci 16:5545–5552. https://doi.org/10.1039/c3cp54910k
51. Jiating H, Bin X, Feipeng C et al (2009) Aggregation-induced emission in the crystals of 9,10-distyrylanthracene derivatives: the essential role of restricted intramolecular torsion. J Phys Chem C 113:9892–9899. https://doi.org/10.1021/jp900205k
52. Edison TNJI, Atchudan R, Shim JJ, Kalimuthu S, Ahn BC, Lee YR (2016) Turn-off fluorescence sensor for the detection of ferric ion in water using green synthesized N-doped carbon dots and its bioimaging. J Photochem Photobiol B Biol 158:235–242. https://doi.org/10.1016/j.jphotobiol.2016.03.010
53. Khateb F, Khatib N, Kubánek D (2012) Low-voltage ultra-low-power current conveyor based on quasi-floating gate transistors. Radioengineering 21:725–735. https://doi.org/10.4103/2229-5186.79345
54. Önal E, Ay Z, Yel Z, Ertekin K, Gürek AG, Topal SZ, Hirel C (2016) Design of oxygen sensing nanomaterial: synthesis, encapsulation of phenylacetylide substituted Pd(II) and Pt(II) meso-tetraphenylporphyrins into poly(1-trimethylsilyl-1-propyne) nanofibers and influence of silver nanoparticles. RSC Adv 6:9967–9977. https://doi.org/10.1039/c5ra24817e
55. Geng T, Huang R, Wu D (2014) Turn-on fluorogenic and chromogenic detection of Fe3+and Cr3+in a completely water medium with polyacrylamide covalently bonding to rhodamine B using diethylenetriamine as a linker. RSC Adv 4:46332–46339. https://doi.org/10.1039/c4ra08640f
56. García-Beltrán O, Cassels BK, Pérez C, Mena N, Núñez M, Martínez N, Pavez P, Aliaga M (2014) Coumarin-based fluorescent probes for dual recognition of copper(II) and iron(III) ions and their application in bio-imaging. Sensors (Switzerland) 14:1358–1371. https://doi.org/10.3390/s140101358
57. Pan C, Wang K, Ji S, Wang H, Li Z, He H, Huo Y (2017) Schiff base derived Fe3+−selective fluorescence turn-off chemsensors based on triphenylamine and indole: synthesis, properties and application in living cells. RSC Adv 7:36007–36014. https://doi.org/10.1039/c7ra05064j
58. Zhao JL, Tomiyasu H, Ni XL, Zeng X, Elsegood MRJ, Redshaw C, Rahman S, Georghiou PE, Yamato T (2014) Synthesis and evaluation of a novel ionophore based on a thiacalix[4]arene derivative bearing imidazole units. New J Chem 38:6041–6049. https://doi.org/10.1039/c4nj01099j
59. Cramer CJ (2004) Essentials of computational chemistry theories and models, 2nd ed. John Wiley & Sons ltd
60. Lewars E (2004) Computational chemistry introduction to the theory and applications of molecular and quantum mechanics. Kluwer Academic Publishers
61. Becke AD (1993) Density-functional thermochemistry. III. The role of exact exchange. J Chem Phys 98:5648–5652
62. Lee C, Yang W, Parr RG (1988) Development of the Colle-Salvetti correlation-energy formula into a functional of the electron density. Phys Rev B 37:785–789
63. Frisch MJ, Trucks GW, Schlegel HB, et al (2009) GAUSSIAN 09 (Revision A.2) Gaussian, Inc., Wallingford, CT
64. R. D. Dennington, T. A. Keith and JMM (2008) , GaussView 5. 0. 8. Gaussian
65. Kaya EN, Yuksel F, Özpinar GA et al (2014) 7-Oxy-3-(3,4,5-trimethoxyphenyl)coumarin substituted phthalonitrile derivatives as fluorescent sensors for detection of Fe3+ ions: experimental and theoretical study. Sensors Actuators B Chem 194:377–388. https://doi.org/10.1016/j.snb.2013.12.044
66. Thasnim P, Bahulayan D (2017) Peptidomimetics as inhibitors of human breast cancer cell line MCF-7. New J Chem 41:13483–13489. https://doi.org/10.1039/c7nj02712e
67. Boo BH, Kim JH (2013) Fluorescence and fluorescence excitation spectroscopy of 5, 8-Dihydroxy-1 , 4-naphtho- quinone . Analysis of the electronic spectra via the time-dependent DFT calculation. Bull Kor Chem Soc 34:309–312
68. Wong ZC, Fan WY, Chwee TS (2018) Computational modelling of singlet excitation energy transfer: a DFT/TD-DFT study of the ground and excited state properties of a *syn* bimane dimer system using non-empirically tuned range-separated functionals. New J Chem 42:13732–13743. https://doi.org/10.1039/C8NJ02920B